

Article

The Ameliorating Effect of *Lizhong-Tang* on Antibiotic-Associated Imbalance in the Gut Microbiota in Mouse

Hye-Ri Ahn ^{1,†}, Do Hwi Park ^{2,†}, Myoung-Sook Shin ² , Quynh Nhu Nguyen ², Jun Yeon Park ³, Dong-Wook Kim ⁴ , Ki Sung Kang ^{2,*} and Hye Lim Lee ^{1,*}

¹ Department of Pediatrics, College of Korean Medicine, Daejeon University, Daejeon 34520, Korea; hyeli23@naver.com

² College of Korean Medicine, Gachon University, Seongnam 13120, Korea; parkdo@gachon.ac.kr (D.H.P.); ms.shin@gachon.ac.kr (M.-S.S.); quynhnhunguyen.nnq@gmail.com (Q.N.N.)

³ Department of Food Science and Biotechnology, Kyonggi University, Suwon 16227, Korea; rhemf@hanmail.net

⁴ College of Pharmacy, Wonkwang University, Iksan 54538, Korea; pharmengin@gmail.com

* Correspondence: kkang@gachon.ac.kr (K.S.K.); hanilim@dju.kr (H.L.L.); Tel.: +82-31-750-5402 (K.S.K.)

† These authors contributed equally to this work.

Abstract: Some herbal medicines have anti-inflammatory and anti-diarrheal effects. This study analyzed the modulating effect of gut microbiota of anti-inflammatory herbal medicines on antibiotic-associated diarrhea (AAD). The anti-inflammatory effects of 10 herbal medicines and *Lizhong-tang* active compounds were studied by measuring the nitric oxide production in an in vitro experiment. This was followed by an in vivo experiment in which the anti-diarrheal effects of *Lizhong-tang* and *Magnolia officinalis* in a lincomycin-induced AAD mouse model were measured. Changes in the intestinal microflora were observed using terminal restriction fragment length polymorphism analysis. Both *Lizhong-tang* and *M. officinalis* were effective against AAD, with *Lizhong-tang*'s anti-diarrheal effects being particularly effective. In addition, the active compounds of *Lizhong-tang*, liquiritin and 6-gingerol, inhibited the expression of inducible nitric oxide synthase and cyclooxygenase-2, thus showing an anti-inflammatory effect. Gut microbiota analysis showed that *Lizhong-tang* could alter the composition of the gut microbiota and ameliorated imbalance in the gut microbiota in a lincomycin-induced AAD mouse model.

Keywords: herbal medicine; *Lizhong-tang*; gut microbiota; anti-inflammatory



Citation: Ahn, H.-R.; Park, D.H.; Shin, M.-S.; Nguyen, Q.N.; Park, J.Y.; Kim, D.-W.; Kang, K.S.; Lee, H.L. The Ameliorating Effect of *Lizhong-Tang* on Antibiotic-Associated Imbalance in the Gut Microbiota in Mouse. *Appl. Sci.* **2022**, *12*, 6943. <https://doi.org/10.3390/app12146943>

Academic Editors: Adriana Basile, Sergio Sorbo, Viviana Maresca and Natália Cruz-Martins

Received: 22 April 2022

Accepted: 6 July 2022

Published: 8 July 2022

Publisher's Note: MDPI stays neutral with regard to jurisdictional claims in published maps and institutional affiliations.



Copyright: © 2022 by the authors. Licensee MDPI, Basel, Switzerland. This article is an open access article distributed under the terms and conditions of the Creative Commons Attribution (CC BY) license (<https://creativecommons.org/licenses/by/4.0/>).

1. Introduction

Intestinal microbes constitute a community of various bacterial phyla that influence the health of the human body by locally affecting nutrient absorption, metabolic immunity, and intestinal health [1]. The composition of the intestinal microflora is determined by changes in not only the environmental background of an individual's lifestyle, such as the host's diet, but also the genetic background and prevalent diseases, such as obesity, intestinal disease, autoimmune disease, and allergy [2]. Newborns are born with low levels of gut microbiome, and exposure to microbes, gradually through childbirth and lactation, leads to the formation of the gut microbiome. Therefore, infants have an incomplete gut microbiome. In addition, compared to adults, children have a weaker gastrointestinal immune system, resulting in frequent digestive system diseases [3–6]. Intestinal microbes influence the structure and function of the immune system of weak digestive organs by acting as a barrier in the gastrointestinal tract through the induction of the expression of proteins necessary to maintain the structure of the intestinal epithelial villi. Therefore, the diversity and settlement of intestinal microbes in children directly affects their health from infancy to adolescence, and gut microbes play an important long-term role in children [7,8].

Antibiotics are drugs used to treat bacterial infections by killing bacteria or inhibiting their growth. With the development of antibiotics, human mortality and life expectancy

due to infectious diseases has improved; however, side effects such as antibiotic-resistant strains appearing due to the exploitation and overuse of antibiotics, reduced compliance with antibiotics, and diarrhea have also been observed [9–12]. Notably, according to the 2021 Organization for Economic Co-operation and Development (OECD), the domestic antibiotic use in Korea was 26.1 daily doses per 1000 inhabitants per day (DID), which was higher than the OECD average of 19.1 DID, and reportedly the third-highest among OECD countries [12]. The most common side effect of antibiotic use is antibiotic-associated diarrhea (AAD), which disrupts the intestinal microbial ecosystem and causes an imbalance in the intestinal microbiota, leading to symptoms of diarrhea.

An imbalance in the gut microbiome can exert negative health effects. Locally, it increases the sensitivity of the intestine and by affecting homeostasis, is also associated with diseases such as obesity (due to systemic metabolic disorders), allergies, and autoimmune diseases [13–15].

AAD, a major symptom during antibiotic treatment, is associated with intestinal microbiome imbalance, inflammation, and changes in intestinal structure. So, we confirmed the inflammation-related factors iNOS, NO, Cox-2, MAPKs, and NF- κ B in Raw 264.7 cells, and observed changes in the intestinal microflora in animal experiments.

Herbal medicines contain small molecules that can be absorbed by the intestine. Herbal medicines can cause physiological changes in the body by affecting intestinal microflora [14]. Therefore, further studies have to investigate whether herbal medicine treatment can preserve and regulate the diversity of the intestinal microflora. Studies on antibiotics and herbal medicines related to intestinal microbes, such as Shen Ling Bai Zhu San [16], Qiweibaizhu [17], ginseng [18], and *Schisandra chinensis* [19], have already been conducted. In this present study, we investigated the effects of herbal medicines on the improving of antibiotic-mediated imbalance of intestinal microflora to evaluate the potential of Eastern medicine.

2. Materials and Methods

2.1. Plant Material

In this study, we tested 10 herbal medicines (3 prescription drugs and 7 plant-based herbal medicines). The prescriptions were *Lizhong-tang*, *Osuyu-tang*, and *Oryeong-san*. *Lizhong-tang* consists of *Panax ginseng*, *Atractylodes lancea*, *Zingiber officinale* Rosc, and *Glycyrrhiza glabra*; *Osuyu-tang* consists of osuyu, *Zingiber officinale*, *Panax ginseng*, and *Ziziphus jujuba* Mill; and *Oryeong-san* consists of *Alisma canaliculatum*, *Poria cocos*, *Crepidiastrum platyphyllum*, and *Magnolia officinalis*. The seven herbal medicines tested included *Paeoniae radix*, *Atractylodes lancea*, *Coicis semen*, *Angelica dahurica*, *Cinamomum cassia*, *Saussurea lappa*, and *Magnolia officinalis*. Herbal medicines were purchased from the Department of Pharmacy, Cheonan Oriental Medicine Hospital, Daejeon University, Korea. For the three prescriptions, the amount of medicinal ingredients was formulated according to the ratio of the existing medicinal ingredients, by referring to Bang-Yak-Hap-Pyun [20] and Donguibogam [21]. *Lizhong-tang* contained 24 g of *Panax ginseng*, 24 g of *Atractylodes lancea*, 24 g of *Zingiber officinale* Rosc, and 12 g of *Glycyrrhiza glabra*. *Osuyu-tang* contained 12 g of osuyu, 9 g of *Atractylodes lancea*, 6 g of *Panax ginseng*, and 4.5 g of *Ziziphus jujuba* Mill. *Oryeong-san* contained 30 g of *Alisma canaliculatum*, 18 g of *Poria cocos* and *Atractylodes lancea*, 18 g of *Polyporus umbellatus*, and 6 g of *Cinamomum cassia*. In total, 40 g of each of the seven herbal medicines was used. The medicinal material was extracted by boiling the herbs in 1000 mL of water at 100 °C for 150 min.

2.2. Isolation of Compounds

Based on the results of a quantitative analysis of the active compounds of *Lizhong-tang* [22], ginsenoside Rb1 and ginsenoside Rg1 from ginseng, 6-gingerol from *Zingiber officinale* Rosc, and liquiritin-glycyrrhizin from *Glycyrrhiza glabra* were selected as representative ingredients. Ginsenoside Rb1, ginsenoside Rg1, and liquiritin were isolated from

Panax ginseng, while 6-gingerol and glycyrrhizin were supplied by the Natural Material Bank (NIKOM).

2.3. Cell Culture

The mouse macrophage cell line, RAW 264.7 (American Type Culture Collection, Rockville, MD, USA), was cultured in DMEM (Manassas, VA, USA) containing 4 mM L-glutamine, antibiotics (1% penicillin/streptomycin), and 10% fetal bovine serum, in a humidified air environment with 5% CO₂, at 37 °C.

2.4. Cell Viability Assay

RAW 264.7 cells were inoculated into 96-well plates at a density of 5×10^4 cells/well for 24 h, and then treated with different concentrations of the samples. To evaluate the effect of the samples on the viability of RAW 264.7 cells, after 24 h of incubation, the cells were tested using a 10% Ez-Cytox Cell Viability Assay Kit (Daeil Lab Service, Seoul, Korea). Cell viability was evaluated by measuring the optical density (OD) at a wavelength of 450 nm using a microplate spectrophotometer (PowerWave™ XS, Bio-Tek Instruments, Winooski, VT, USA).

2.5. Western Blot Analysis

RAW 264.7 cells were seeded into 6-well plates at a density of 1×10^6 cells/well. After incubation for 24 h, the cells were treated with samples in the treatment medium, as described previously. After 20 h of treatment with lipopolysaccharide (LPS), the cells were washed with Dulbecco's phosphate-buffered saline (Welgene Inc., Daegu, Korea). Subsequently, the cells were harvested and lysed in $1 \times$ radioimmunoprecipitation assay buffer (Tech & Innovation, Gangwon, Korea) supplemented with a proteinase inhibitor cocktail (Roche Diagnostics, Basel, Switzerland) to obtain whole-cell extracts. Proteins in the cell extracts of each sample were quantified using a Pierce BCA Protein Assay Kit (Thermo Fisher Scientific, Waltham, MA, USA). Equal amounts of proteins (20 µg/lane) were separated using 10% sodium dodecyl sulfate-polyacrylamide gel electrophoresis and transferred onto polyvinylidene difluoride membranes. The membranes were then blocked with 5% skim milk in Tris-buffered saline (1×) for 1 h, following which the separated proteins were identified through incubation with epitope-specific primary and secondary antibodies (Cell Signaling Technology, Danvers, MA, USA). The membranes were visualized using SuperSignal™ West Femto Maximum Sensitivity Substrate (Thermo Fisher Scientific, Waltham, MA, USA) and imaged using a FUSION Solo Chemiluminescence System (Vilber Lourmat Deutschland GmbH, Eberhardzell, Germany).

2.6. In Vivo AAD Model Generation and Treatment Experiments

The in vivo investigations were supported by the Institutional Animal Care and Use Committee (Internal Review Board deliberation number: KBI0-IACUC-2018-106). BALB/c mice (6-weeks-old), with an average body weight of 20–21 g, supplied by Daehan Biolink (Chungcheongbuk-do, Korea) were used in the experiment. The animals were maintained in a room under standard laboratory condition with a 12:12 h light–dark cycle with a constant temperature of 22 ± 2 °C and humidity of $55 \pm 10\%$. All animals were alive until the end of the experiment, and after the end of the experiment, they were anesthetized and euthanized. All procedures involving animals throughout the experiments were conducted in strict accordance with the legislation on the use and care of laboratory animals. Moreover, all efforts were made to minimize suffering. After 7 d of acclimatization, a total of four groups ($n = 5$ /group) were tested: control group, untreated group (normal), and two experimental groups (sample 1: *Lizhong-tang*; sample 2: *M. officinalis*). To establish the AAD model, lincomycin was orally administered to the animals at a dosage of 3 g/kg, twice daily (8 h apart) for 7 d. The untreated group (normal) was administered the same amount of physiological saline without lincomycin. After constructing the AAD model, a 10 mL/kg sample (*M. officinalis* or *Lizhong-tang*) was administered to the experimental group (sample)

twice a day, while the control group was administered saline twice daily. The body weight, water intake, and diarrhea (diarrheal status score) were assessed for all the groups. At the end of the experiment, animals were first anesthetized using 2% isoflurane O₂ inhalation, and the intestinal tissues were dissected and their fecal contents were collected under sterile conditions and stored at −80 °C. The stored tissues were analyzed for diversity and community structure of the gut microbiota using terminal restriction fragment length polymorphism (T-RFLP) (Figure 1).

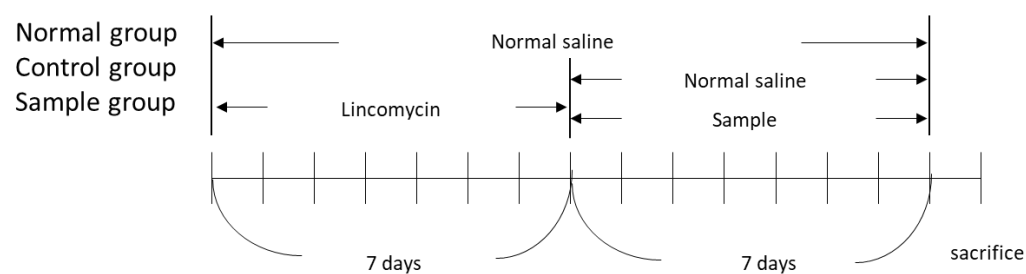


Figure 1. Schedule of the in vivo experiment to induce an antibiotic-associated diarrhea model in BALB/c mice.

2.7. Gene Expression Analysis Using Quantitative Real-Time Polymerase Chain Reaction (qRT-PCR)

DNA was extracted from the dissected intestinal tissue contents, homogenized through bead beating using Precellys[®] 24 (Bertin, Montigny-le-Bretonneux, France), and purified using the High Pure PCR Template Preparation Kit (Roche Diagnostics). The primers used included 5'-FAM-labeled 35f (5'-CCTGGCTCAGGATGAACG-3'; *E. coli* positions 35–52) and 1492r (5'-GGTTACCTTGTTACGACTT-3'; *E. coli* positions 1510–1492). Amplification was performed using A-Star Lamp Taq DNA Polymerase (BioFACT[™], Seoul, Korea) for 30 cycles at 95 °C for 3 min, 95 °C for 30 s, 55 °C for 60 s, 72 °C for 30 s, and 70 °C for 10 min. The PCR products were purified using the HiGene[™] Gel & PCR Purification System (BioFACT[™]) (Table 1). The purified PCR products were digested with the restriction endonuclease, MspI (Thermo Fisher Scientific), and fragment analysis was performed using an ABI PRISM 3130xl genetic analyzer (Applied Biosystems, Waltham, MA, USA). The DNA size marker used was MM-ROX X-Rhodamine (BioVentures, Wellesley, MA, USA). Fragment size, peak height, and area were analyzed using GeneMapper[®] software (version 3.0; Applied Biosystems).

Table 1. Primer sequences for quantitative real-time polymerase chain reaction.

Primer Sequence	Product Size (bp)
¹ Forward: 5'-CCTGGCTCAGGATGAACG-3'	approximately 1500
¹ Reverse: 5'-GGTTACCTTGTTACGACTT-3'	
² Forward: 5'-CCTTAAACAGGCCCACTTGA-3'	approximately 1400 GAPDH
² Reverse: 5'-CCTTCCACAATGCCAAAGTT-3'	

¹ The 16S rRNA genes were amplified using the primers, 5' FAM-labeled 35f (5'-CCTGGCTCAGGATGAACG-3') and 1510r (5'-GGTTACCTTGTTACGACTT-3'); ² The rRNA genes housekeeping gene (5'-CCTTAAACAGGCCCACTTGA-3') and (5'-CCTTCCACAATGCCAAAGTT-3').

2.8. Measurement of Nitric Oxide (NO) Produced by RAW 264.7 Cells

An NO assay was conducted to assess the ability of the samples to inhibit NO secretion. After 2 h of sample treatment, the cells were stimulated with 100 ng/mL LPS from *Escherichia coli* O26:B6 (Sigma-Aldrich, St. Louis, MO, USA). After 20 h of stimulation, the supernatant of the cultured cells was incubated with the same amount of Griess reagent. NO concentration was evaluated by measuring the OD at the wavelength of 550 nm using a microplate spectrophotometer.

2.9. Statistical Analysis

All data are presented as mean \pm standard deviation (SD). Statistical significance was determined using one-way analysis of variance and multiple comparisons with Bonferroni correction. Statistical significance was set at a p value < 0.05 . All analyses were performed using SPSS Statistics ver. 19.0 (IBM, Chicago, IL, USA).

3. Results

3.1. Effect of Herbal Extracts on LPS-Induced NO Production in RAW 264.7 Cells

NO plays many important roles in the immune system. Specially, NO is produced in high amounts in macrophages to respond to stimulation. To investigate the anti-inflammatory effect of the 10 extracts, the inhibitory effect of the extracts 1–10 on NO production in LPS-activated RAW 264.7 macrophages was measured. In addition to evaluating their cytotoxicity in RAW 264.7 cells, cell viability was observed. At non-cytotoxic concentrations, 8 out of the 10 extracts caused a significant reduction in NO production in LPS-activated RAW 264.7 cells. These eight extracts included the herbal extracts *Lizhong-tang* and *M. officinalis*. Compared to those in the LPS-treated group ($9.48 \pm 0.30 \mu\text{M}$), the NO levels in the co-culture with *Lizhong-tang* (12.5, 25, 50, and 100 μM) and LPS were significantly lower, at $7.81 \pm 0.26 \mu\text{M}$, $8.48 \pm 0.13 \mu\text{M}$, $7.59 \pm 0.13 \mu\text{M}$, and $2.70 \pm 0.10 \mu\text{M}$, respectively (Figure 2). Similarly, *M. officinalis* (50 μM and 100 μM) extracts significantly reduced the NO levels to $6.59 \pm 0.10 \mu\text{M}$ and $1.15 \pm 0.10 \mu\text{M}$, respectively, as compared to those in the LPS-treated group ($9.48 \pm 0.30 \mu\text{M}$). These results suggest that *Lizhong-tang* and *M. officinalis* may have anti-inflammatory activities in LPS-activated RAW 264.7 cells. Considering the cell viability results after treatment with *Lizhong-tang* and *M/officinalis*, it was observed that the inhibitory effect on NO levels in LPS-activated RAW 264.7 cells was not due to cytotoxicity.

3.2. Evaluation of the Inhibitory Activity of the Active Compounds of *Lizhong-Tang* on LPS-Induced NO Production in RAW 264.7 Cells

To determine the NO-inhibitory effects of the active compounds of *Lizhong-tang*, NO assays were carried out post-treatment of RAW 264.7 cells with the six compounds from *Lizhong-tang*, including liquiritin, ginsenoside Rb1, ginsenoside Rg1, glycyrrhizin, and 6-gingerol. Liquiritin, ginsenoside Rg1, glycyrrhizin, and 6-gingerol significantly reduced the NO levels in the LPS-stimulated RAW 264.7 cells. Of these compounds, liquiritin and 6-gingerol were the most effective at non-cytotoxic concentrations.

No cytotoxicity was observed at all the tested concentrations of liquiritin (12.5, 25, 50, and 100 μM), similar to that in the untreated group. In the group stimulated with 100 ng/mL LPS, the NO levels were $21.52 \pm 0.42 \mu\text{g/mL}$, while in the experimental group treated with 12.5 μM liquiritin, the NO levels decreased compared to those in the group stimulated with LPS to $20.19 \pm 0.34 \mu\text{g/mL}$; this decrease, however, was not significant. In the group treated with 25 μM , 50 μM , and 100 μM liquiritin, NO levels were $19.33 \pm 0.27 \mu\text{g/mL}$, $14.33 \pm 0.13 \mu\text{g/mL}$, and $7.19 \pm 0.14 \mu\text{g/mL}$, respectively, which represented an inhibition ($p < 0.001$) of the NO levels in the LPS-stimulated group (Figure 3).

For ginsenoside Rb1, no cytotoxicity was observed at the 12.5, 25, 50, and 100 μM , concentrations similar to that seen in the untreated group. In the group stimulated with 100 ng/mL LPS, the NO levels were $21.52 \pm 0.42 \mu\text{g/mL}$, while that in the experimental groups treated with 12.5, 25, 50, and 100 μM ginsenoside Rb1 were $21.48 \pm 0.05 \mu\text{g/mL}$, $21.57 \pm 0.25 \mu\text{g/mL}$, $21.24 \pm 0.17 \mu\text{g/mL}$, and $22.33 \pm 0.05 \mu\text{g/mL}$, respectively (Figure 3). Thus, no significant change was observed in the NO levels, after treatment with Rb1 at any of the concentrations tested. No cytotoxicity was observed at all concentrations of ginsenoside Rg1 (12.5, 25, 50, and 100 μM), similar to that seen in the untreated group. In the group stimulated with 100 ng/mL LPS, the NO levels were $21.52 \pm 0.42 \mu\text{g/mL}$, while in the experimental group treated with 12.5 μM of ginsenoside Rg1, there was no significant change, with the NO levels at $20.81 \pm 0.33 \mu\text{g/mL}$. In the group treated with 25 μM ginsenoside Rg1, the NO levels decreased to $20.00 \pm 0.22 \mu\text{g/mL}$ ($p < 0.05$). The

NO levels decreased ($p < 0.001$) (Figure 3) in the groups treated with 50 μM and 100 μM ginsenoside Rg1 to $16.76 \pm 0.17 \mu\text{g}/\text{mL}$ and $8.10 \pm 0.29 \mu\text{g}/\text{mL}$, respectively.

No cytotoxicity was observed at all concentrations (12.5, 25, 50, and 100 μM) of glycyrrhizin, similar to that seen in the untreated group. In the group stimulated with 100 ng/mL LPS, the NO levels were $21.52 \pm 0.42 \mu\text{g}/\text{mL}$, while in the experimental group treated with 12.5 μM glycyrrhizin, there was no significant change in the NO levels at $21.29 \pm 0.22 \mu\text{g}/\text{mL}$. In the group treated with 25 μM glycyrrhizin, the NO levels decreased to $20.33 \pm 0.17 \mu\text{g}/\text{mL}$, but the difference was not statistically significant. NO levels reduced ($p < 0.001$) to $17.33 \pm 0.34 \mu\text{g}/\text{mL}$ and $11.67 \pm 0.60 \mu\text{g}/\text{mL}$ in the groups treated with 50 μM and 100 μM glycyrrhizin, respectively (Figure 3). No cytotoxicity was observed at concentrations of 12.5, 25, 50, and 100 μM 6-gingerol, similar to that seen in the untreated group. In the group stimulated with 100 ng/mL LPS, the NO levels were $20.67 \pm 0.27 \mu\text{g}/\text{mL}$, while in the groups treated with 12.5 μM , 25 μM , 50 μM , and 100 μM 6-gingerol, there was a decrease ($p < 0.001$) in the NO levels to $13.62 \pm 0.17 \mu\text{g}/\text{mL}$, $11.14 \pm 0.80 \mu\text{g}/\text{mL}$, $8.57 \pm 0.43 \mu\text{g}/\text{mL}$, and $4.76 \pm 0.48 \mu\text{g}/\text{mL}$, respectively (Figure 3).

A

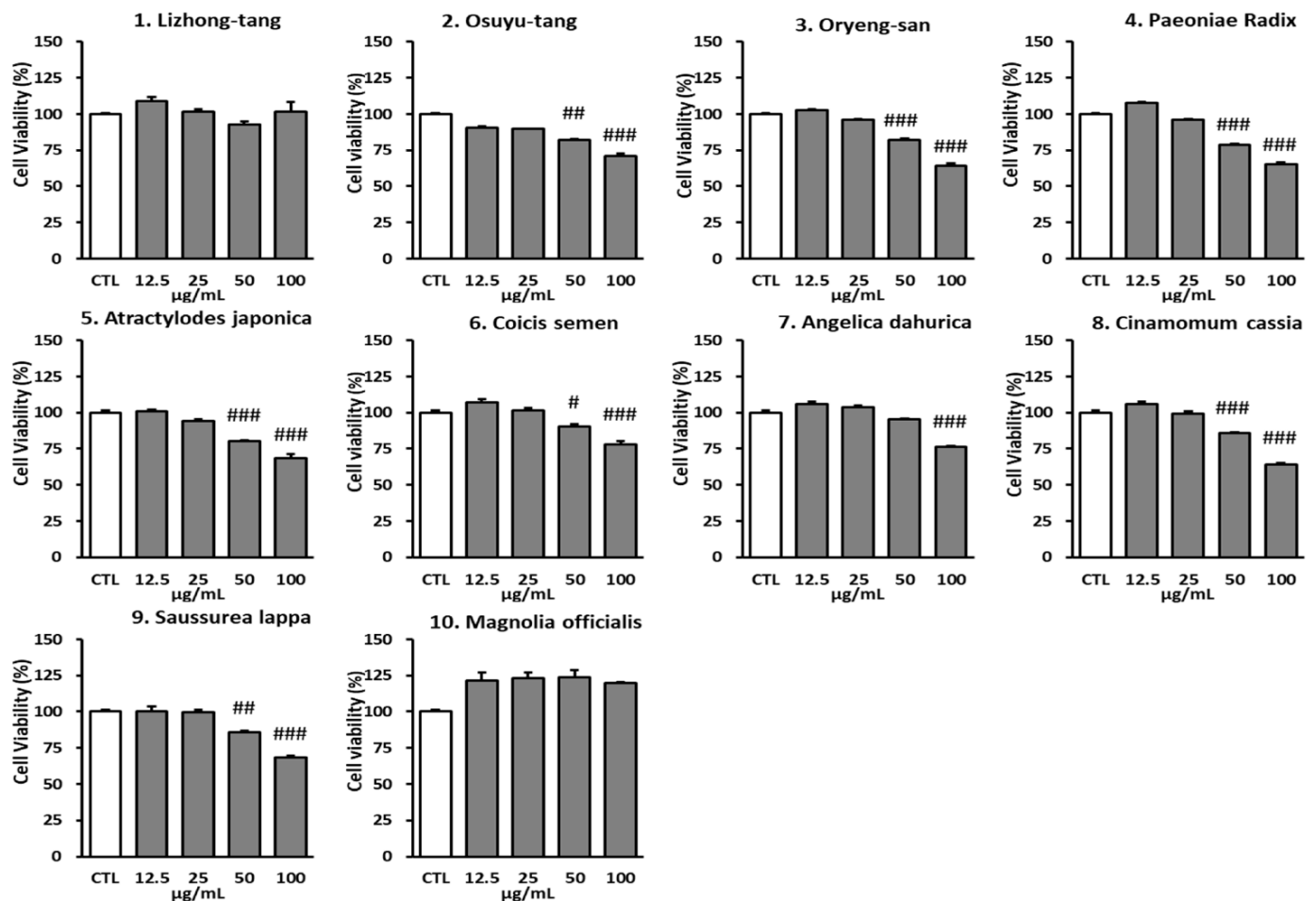


Figure 2. Cont.

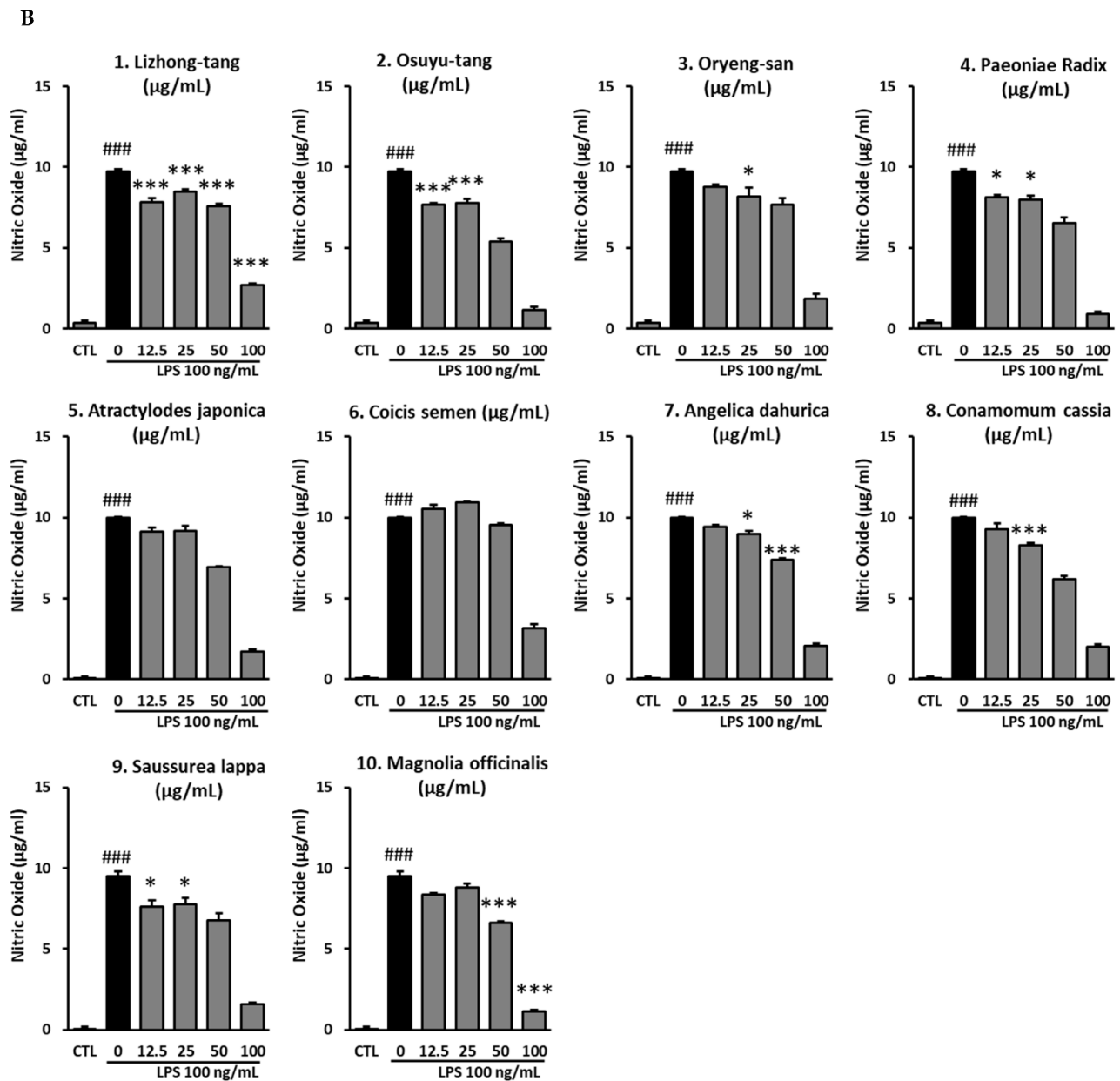


Figure 2. Effects of the 10 extracts on inhibition of nitric oxide (NO) production. RAW 264.7 cells were pre-treated with various concentrations of the 10 extracts. (A): Cytotoxic effects of the 10 extracts. (B): NO production upon treatment with the 10 extracts. Results have been expressed as mean \pm SEM ($n = 3$). Statistical analysis was carried out by means of ANOVA with Tukey's post-hoc test, using software R version 3.3.3. # $p < 0.05$, ## $p < 0.01$, ### $p < 0.001$, compared to the non-treated group; * $p < 0.05$, ** $p < 0.001$, compared to the LPS-treated group.

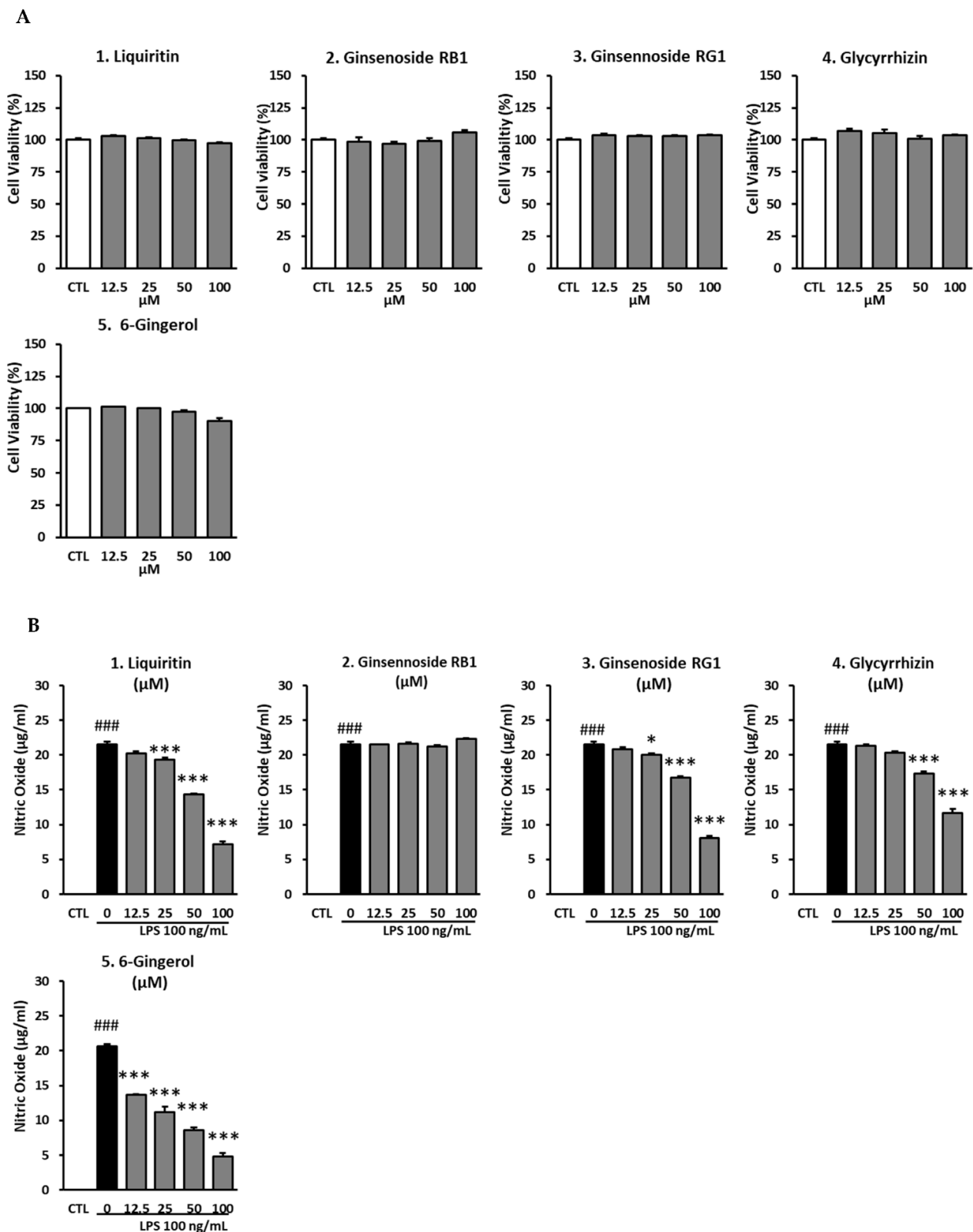


Figure 3. Inhibitory effects of liquiritin, ginsenoside Rb1, ginsenoside Rg1, glycyrrhizin, and 6-gingerol in RAW 264.7 cells. The cells were pre-treated with various concentrations of active compounds from Lishong-tang (liquiritin, ginsenoside Rb1, ginsenoside Rg1, glycyrrhizin, and 6-gingerol). (A): Cytotoxic effects of the active compounds of Lishong-tang. (B): Inhibition of nitric oxide production by the active compounds of Lishong-tang. RAW 264.7 cells were treated with lipopolysaccharide

(LPS; 100 ng/mL) and samples. The data have been represented as mean \pm SEM. Statistical significance was evaluated by means of ANOVA followed by Tukey's post-hoc test, using software R version 3.3.3. ### $p < 0.001$, as compared to the normal group; * $p < 0.05$, and *** $p < 0.001$, as compared to the LPS-treated group.

3.3. Evaluation of Inhibition of LPS-Induced NO Production in RAW 264.7 Cells by a Mixture of Liquiritin and 6-Gingerol

In RAW 264.7 cells, the inhibition of NO production by five active compounds (liquiritin, ginsenoside Rb1, ginsenoside Rg1, glycyrrhizin, and 6-gingerol) was evaluated. Liquiritin and 6-gingerol, which showed the best inhibitory efficacy, were evaluated at the highest concentration of 50 μ M. Following that, the effect of a mixture of liquiritin and 6-gingerol mixture on the inhibition of NO production was also evaluated.

There was no cytotoxicity upon treatment with any concentration of liquiritin (6.25, 12.5, 25, and 50 μ M), similar to that seen in the untreated group. In the group stimulated with 100 ng/mL LPS, the NO levels were 18.48 ± 1.06 μ g/mL, while that in the groups treated with 6.25 μ M and 12.5 μ M liquiritin was decreased to 17.00 ± 0.86 μ g/mL and 15.38 ± 0.85 μ g/mL, respectively; this difference, however, was not significant. In the group treated with 25 μ M liquiritin, there was an inhibition ($p < 0.05$) of the NO levels (14.05 ± 1.46 μ g/mL) compared to those in the LPS-treated group. In the group treated with 50 μ M liquiritin, the NO levels were 10.95 ± 0.31 μ g/mL. The NO levels were suppressed after treatment with 50 μ M ($p < 0.001$) liquiritin, compared to those in the LPS-stimulated group (Figure 4).

No cytotoxicity was observed upon treatment with any concentration of 6-gingerol (6.25, 12.5, 25, and 50 μ M), similar to that in the untreated group. In the group stimulated with 100 ng/mL LPS, the NO levels were 18.48 ± 1.06 μ g/mL, while that in the experimental groups treated with 6.25 μ M and 12.5 μ M 6-gingerol, was reduced ($p < 0.05$) to 13.90 ± 0.25 μ g/mL and 13.90 ± 0.88 μ g/mL, respectively, compared to those in the LPS-treated group. There was a decrease in the NO levels ($p < 0.001$) in the groups treated with higher concentrations of 6-gingerol, (i.e., 25 μ M and 50 μ M), with the NO levels at 11.00 ± 0.38 μ g/mL and 6.62 ± 0.48 μ g/mL, respectively, compared to those in the LPS-stimulated group (Figure 4).

Liquiritin and 6-gingerol were mixed in a 1:1 ratio to reach the final concentrations of 6.25, 12.5, 25, and 50 μ M to evaluate the effect of the mixture on the inhibition of NO production. No cytotoxicity of liquiritin and 6-gingerol was observed at 6.25, 12.5, 25, and 50 μ M, similar to that seen in the untreated group. In the group stimulated with 100 ng/mL LPS, the NO level was 18.48 ± 1.06 μ g/mL, while that in the experimental groups treated with liquiritin and 6-gingerol at 6.25 μ M, 12.5 μ M, and 25 μ M were $14.52.81 \pm 0.25$ μ g/mL, 12.24 ± 0.42 μ g/mL, and 7.43 ± 0.44 μ g/mL, respectively. In the group treated with 50 μ M liquiritin and 6-gingerol, the NO level was 2.24 ± 0.19 μ g/mL, which was lower ($p < 0.001$) than that in the LPS-stimulated group (Figure 4).

3.4. Effects of Liquiritin and 6-Gingerol on LPS-Induced Expression of Mitogen-Activated Protein Kinase (MAPK) Proteins in RAW 264.7 Mouse Macrophages

RAW 264.7 cells were stimulated with LPS and then treated with 50 μ M liquiritin, 20 μ M 6-gingerol, or a mixture of 50 μ M liquiritin and 20 μ M 6-gingerol, following which the expression levels of MAPK proteins were assessed in the cells. In the test on the inhibitory effect of a mixture of liquiritin and 6-gingerol on nitric oxide (NO) production, the most effective concentration of liquiritin was a 1:1 ratio of liquiritin and 6-gingerol, compared with double the concentration at the corresponding concentrations of liquiritin and 6-gingerol alone.

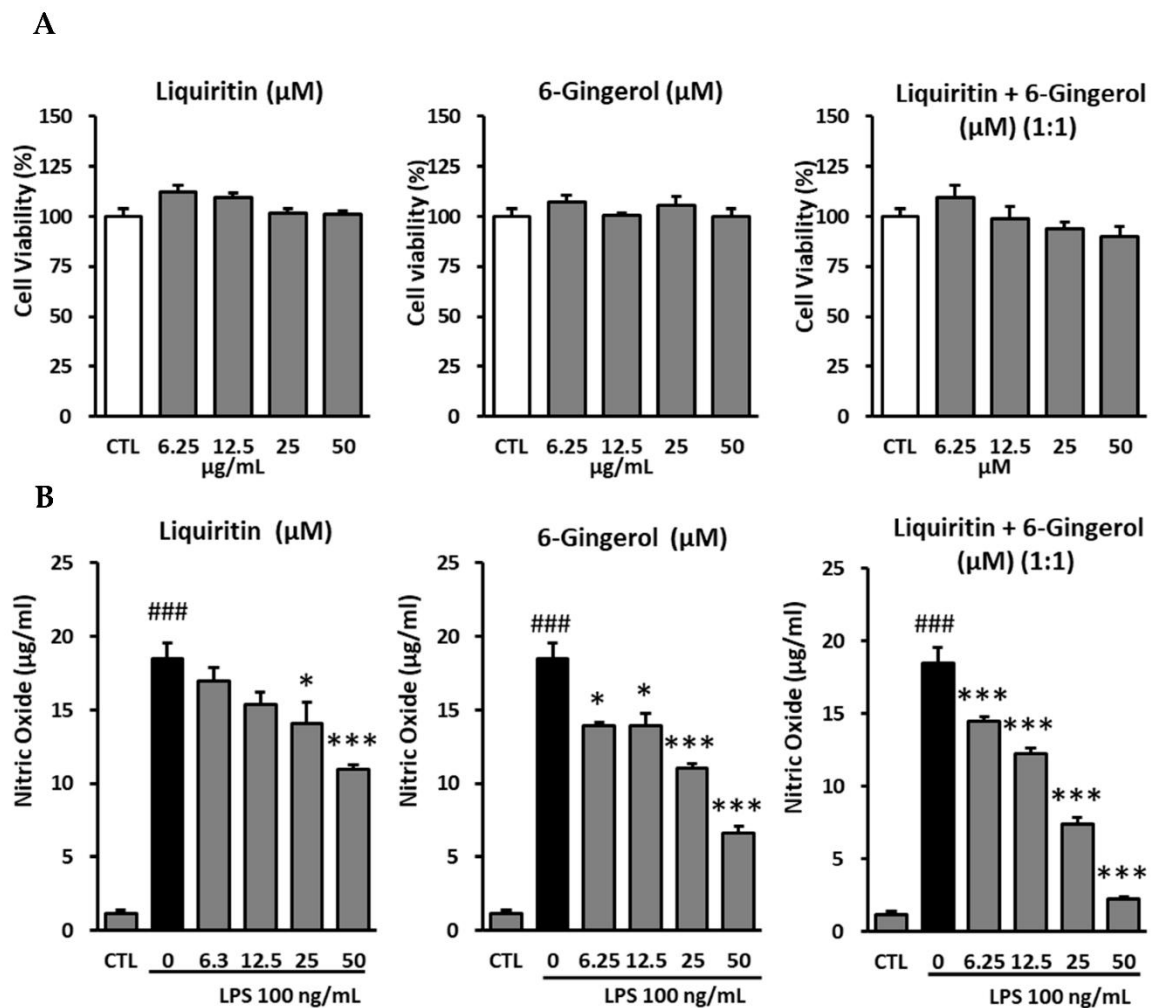


Figure 4. Inhibitory effects of liquiritin and 6-gingerol on RAW 264.7 cells. (A): Cytotoxic effects of liquiritin and 6-gingerol on RAW 264.7 cells. (B): Inhibition of nitric oxide production by liquiritin and 6-gingerol in LPS-mediated RAW 264.7 cells. The cells were pre-treated with various concentrations of liquiritin and 6-gingerol, following which the cells were treated with LPS (100 ng/mL). After 24 h, the nitric oxide levels in the culture medium were measured using Griess reaction. The data are presented as mean \pm SEM. Statistical significance was assessed by means of ANOVA followed by Tukey's post-hoc test, using software R version 3.3.3. ### $p < 0.001$, compared to the normal group; * $p < 0.05$, and *** $p < 0.001$, compared to the LPS-treated group.

The NO concentration in the LPS group was 50 μ M, which is approximately 60% of maximum. For Western blot analysis, 20 μ M 6-gingerol, which resulted in NO levels that were approximately 60% of those in the LPS group, was selected, and a mixture of 50 μ M liquiritin and 20 μ M 6-gingerol was tested. The levels of phosphorylated c-Jun NH2-terminal kinase (p-JNK), phosphorylated extracellular signal-regulated kinase (p-ERK), p-p38, cyclooxygenase-2 (COX-2), and inducible nitric oxide synthase (iNOS) increased upon LPS treatment. There was a decrease in the protein expression levels of p-JNK, p-ERK, p-p38, COX-2, and iNOS in the groups treated with 50 μ M liquiritin alone, as well as 50 μ M liquiritin and 20 μ M 6-gingerol together, post-LPS stimulation. The protein expression levels of p-JNK, p-p38, COX-2, and iNOS also decreased in the group treated with 20 μ M 6-gingerol, post-LPS stimulation. In addition, the group treated with 50 μ M liquiritin and 20 μ M 6-gingerol together showed a significant decrease in protein expression, compared to that in the LPS-stimulated group (Figure 5).

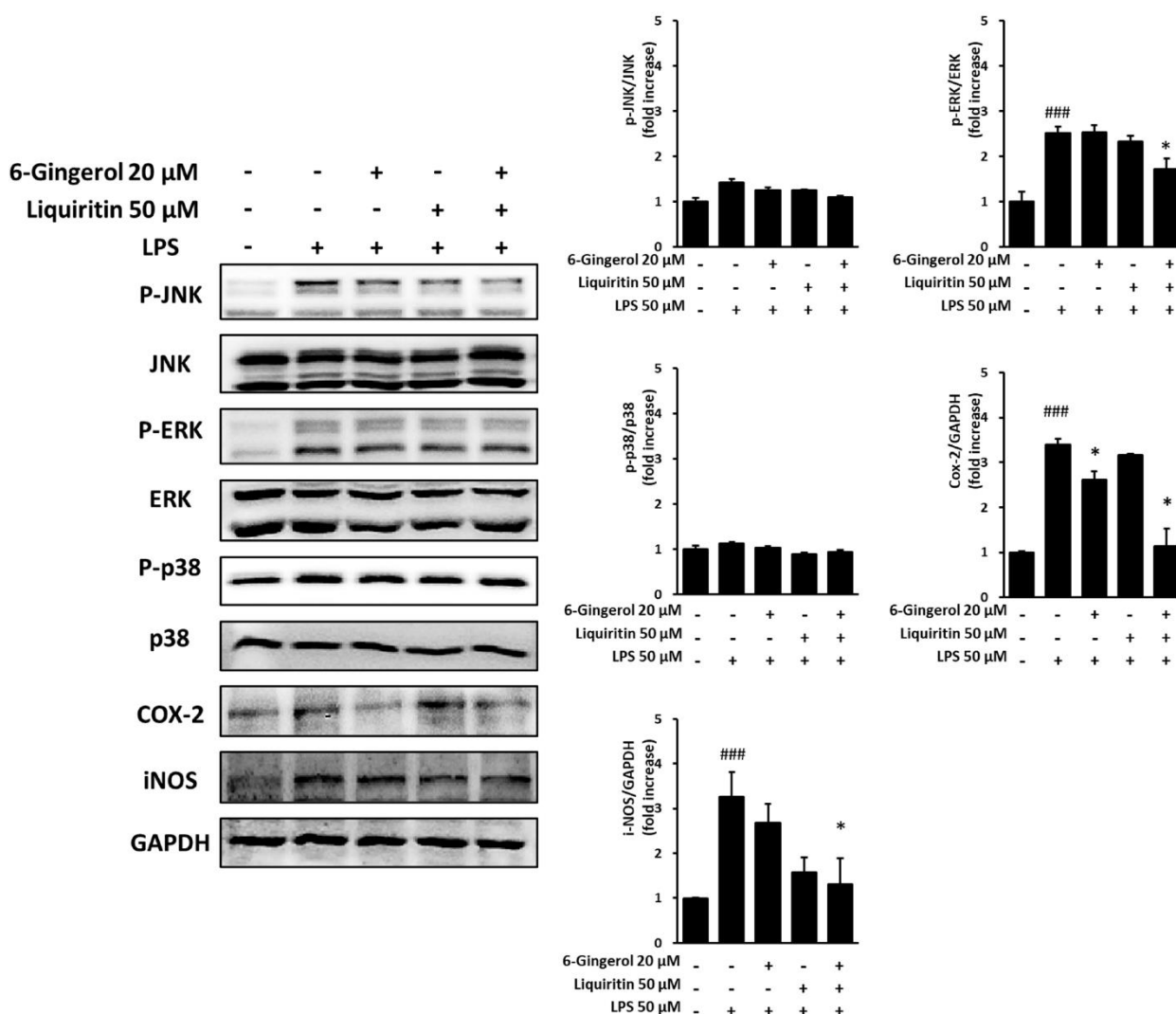


Figure 5. Inhibitory effects of liquiritin and 6-gingerol on the protein expression levels of p-JNK, p-ERK, p-p38, COX-2, and iNOS in RAW 264.7 cells. The cells were pre-treated with various concentrations of liquiritin and 6-gingerol, following which the cells were treated with LPS (100 ng/mL) for 20 h. The phosphorylation levels of p-JNK, p-ERK, p-p38, COX-2, and iNOS were analyzed using Western blot. The data are presented as mean \pm SEM. Statistical significance was assessed by means of ANOVA followed by Tukey’s post-hoc test, using software R version 3.3.3. ### $p < 0.001$, compared to the normal group; * $p < 0.05$, compared to the LPS-treated group.

3.5. Effect of Lizhong-Tang and *M. officinalis* Extracts on AAD Mice

After treating the animals with lincomycin hydrochloride, the rats showed diarrheal symptoms, including lower food consumption, increased water intake, and increased defecation frequency. By the end of the experiment, the animals displayed 100% diarrhea, thus suggesting the successful establishment of an AAD mouse model. After the end of the experiment, all the experimental animals survived. In the untreated group (normal), there was almost no change in body weight, with weight being 100%, 100.32%, 100.50%, and 100.86% on the 1st, 2nd, 3rd, and 4th day, respectively. In the control group taking antibiotics, the weight was 100%, 98.86%, 97.28%, and 95.70% on the 1st, 2nd, 3rd, and 4th day, respectively, that is, the weight gradually decreased over time. In the group administered with *Lizhong-tang*, the weight was 100%, 99.28%, 99.57%, and 100.52% on the 1st, 2nd, 3rd, and 4th day, respectively. The group administered with *M. officinalis* extract showed a tendency to lose weight, with the weight being 100%, 99.28%, 96.12%, and 97.38% on the 1st, 2nd, 3rd, and 4th day, respectively (Table 2).

Table 2. Relative abundance of weight, fluid intake, and diarrhea level in each group.

Change of Body Weight (%)				
Group	Normal	Control	<i>Magnolia Officinalis</i>	<i>Lizhong-Tang</i>
1 day	100 ± 2.31	100 ± 3.57	100 ± 3.31	100 ± 3.24
2 day	100.3 ± 2.46	98.86 ± 4.06	99.27 ± 3.4	98.79 ± 4.21
3 day	100.5 ± 2.4	97.28 ± 5.07	96.11 ± 4.29	99.56 ± 5.21
4 day	100.8 ± 3.26	95.7 ± 4.1	97.3 ± 3.52	100.5 ± 2.74
5 day	101 ± 3.3	95 ± 2.23	96.5 ± 4.0	100.2 ± 3.72
6 day	101.3 ± 3.54	92.9 ± 4.14	94.34 ± 4.14	100.5 ± 3.67
7 day	101.6 ± 2.75	91.45 ± 2.45	93.2 ± 4.3	100.7 ± 2.62
Water intake(mL)				
group	Normal	Control	<i>Magnolia officinalis</i>	<i>Lizhong-tang</i>
1 day	22.2 ± 5.23	22.8 ± 2.54	22.2 ± 2.1	23.2 ± 2.14
2 day	22.3 ± 4.65	22.6 ± 3.24	22 ± 2.54	22.9 ± 3.71
3 day	22.3 ± 3.34	22.2 ± 4.27	21.3 ± 4.28	23.1 ± 4.32
4 day	22.4 ± 2.86	21.8 ± 3.13	21.6 ± 4.12	23.3 ± 3.6
5 day	22.5 ± 4.33	21.5 ± 4.53	21.2 ± 3.24	23.3 ± 2.37
6 day	22.5 ± 5.74	21.2 ± 5.21	20.9 ± 2.64	22.5 ± 4.19
7 day	22.6 ± 2.67	20.9 ± 4.16	20.7 ± 3.73	23.4 ± 3.46
Diarrhea status score				
group	Normal	Control	<i>Magnolia officinalis</i>	<i>Lizhong-tang</i>
1 day	0	10.54 ± 1.2	9.81 ± 1.1	9.95 ± 1.2
2 day	0	7.84 ± 1.4	6.91 ± 1.2	5.6 ± 1.5
3 day	0	7.5 ± 1.5	6.51 ± 1.8	5.5 ± 1.2
4 day	0	6.84 ± 1.2	6.28 ± 1.5	5.24 ± 1.5
5 day	0	5.21 ± 2.2	5.2 ± 1.2	4.53 ± 1.2
6 day	0	5.2 ± 1.2	5.0 ± 1.2	4.12 ± 1.4
7 day	0	4.8 ± 2.2	4.5 ± 1.5	3.2 ± 1.2

Normal group—untreated group; control group—antibiotic-associated diarrhea (AAD) group; *M. officinalis* group—group orally administered with *M. officinalis* extract, post-AAD establishment; *Lizhong-tang* group—group orally administered with *Lizhong-tang*, post-AAD establishment. Values have been expressed as mean ($n = 5$). Statistically significant values were compared against the control by means of one-way ANOVA followed by Tukey's post-hoc test, using the software R version 3.3.3.

The water intake of the untreated group (normal) was 24.9 mL, 20.5 mL, and 21.4 mL on the 2nd, 3rd, and 4th day, respectively. In the control group administered with antibiotics, the water intake increased, compared to that in the untreated group. Compared to that in the control group, the water intake in the group administered with *Lizhong-tang* was not significantly different, but showed a tendency to decrease. Water intake in the *M. officinalis* extract-treated group increased compared to that in the untreated group, but decreased compared to that in the control group; this difference, however, was not statistically significant (Table 2).

The degree of diarrhea in the control group taking antibiotics was 10, 7, and 6 points on the 2nd, 3rd, and 4th day, respectively. The group administered with *Lizhong-tang* had diarrhea scores of 9, 5, and 5 points on the 2nd, 3rd, and 4th day, respectively, which was not significantly different compared to those in the control group, but showed a lower tendency. The group administered with *M. officinalis* scored 9, 6, and 6 points on the 2nd, 3rd, and 4th

day, respectively, which was lower than those in the control group, although not statistically significant, but higher than those in the group administered with *Lizhong-tang* (Table 2).

3.6. Effect of *Lizhong-Tang* on the T-RFLP Profiles of Small Intestinal Contents, Based on Operational Taxonomic Units (OTUs)

T-RFLP analysis was performed on the intestinal tissues containing fecal contents to determine the effect of *Lizhong-tang* on intestinal microflora control, using CNGB (mouse and human) and MICA3.0 (RDP 16S bacterial rRNA) databases. Table 2 shows a database-based list of the bacteria expected to be included in each OTU community (Table 2). By means of T-RFLP analysis, it was found that the intestinal microbial communities of the mice in the untreated (normal), control (control), and *Lizhong-tang*-administered groups were changed substantially. The antibiotics-administered group showed a change in the intestinal microbial community compared to that of the untreated group, while the *Lizhong-tang*-administered group showed a change in the intestinal microbial community compared to that of the control group. This indicated the similarity within each group and the independence between the three groups, indicating successful establishment of the AAD model (Figure 6). The untreated group had the highest contents of OTU548 and OTU558 (Table 3). The control group showed an increase in OTU485, but its content of OTU558 and OTU548 decreased, compared to that in the untreated group (normal). The *Lizhong-tang*-administered group showed an increase in the OTU147 and OTU133 content, compared to that in the control group (Figures 7 and 8).

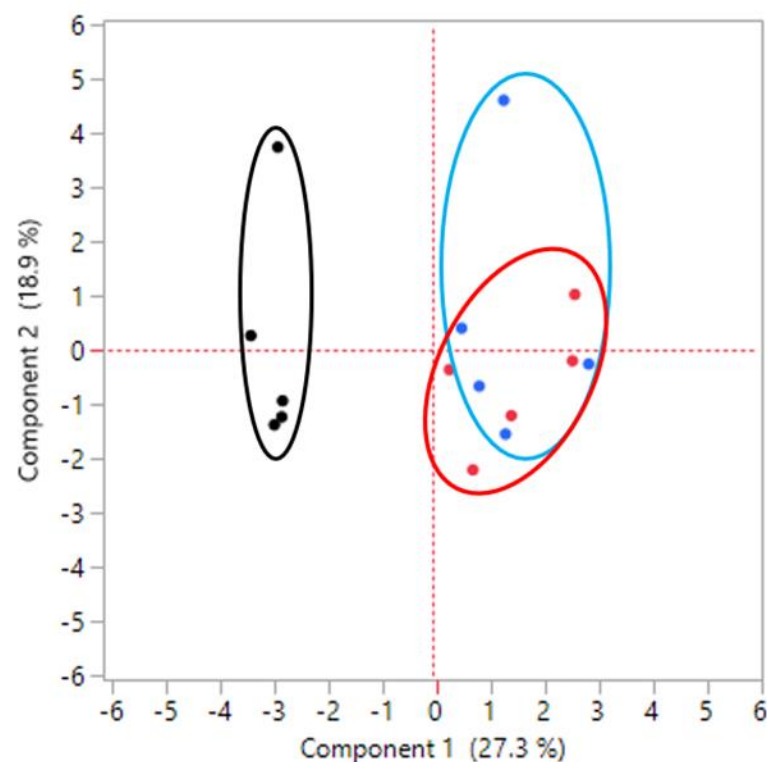


Figure 6. Principal component analysis showing the difference in the small intestinal microbiota composition between groups. Black dot: normal group, without treatment. Blue dot: control group, with antibiotic-associated diarrhea (AAD). Red dot: sample group, *Lizhong-tang*-administered group, post-AAD establishment.

Table 3. Correspondence of OTUs to the bacteria predicted by means of theoretical digestion with the restriction endonuclease, MspI.

	OTU	Predicted Bacteria from T-RFLP
39	ND	
45	ND	
101	<i>Prevotella ruminicola</i> <i>Alistipes finegoldii</i> <i>Bacteroides fragilis</i> <i>Bacteroides helcogenes</i> <i>Bacteroides salanitronis</i>	<i>Bacteroides thetaiotaomicron</i> <i>Bacteroides vulgatus</i> <i>Odoribacter splanchnicus</i> <i>Parabacteroides distasonis</i> <i>Prevotella ruminicola</i>
133	<i>Bifidobacterium bifidum</i> <i>Bifidobacterium longum</i> <i>Bacillus anthracis</i> <i>Bacillus cereus</i> <i>Bacillus thuringiensis</i>	<i>Bifidobacterium breve</i> <i>Bacillus subtilis</i> <i>Bifidobacterium bifidum</i> <i>Listeria innocua</i>
147	<i>Eubacterium eligen</i> <i>Staphylococcus aureus</i>	
164	<i>Lactobacillus acidophilus</i> <i>Lactobacillus crispatus</i> <i>Finegoldia magna</i> <i>Lactobacillus amylovorus</i>	<i>Lactobacillus delbrueckii</i> <i>Lactobacillus acidophilus</i> <i>Lactobacillus crispatus</i> <i>Lactobacillus helveticus</i>
183	ND	
195	<i>Ruminococcus obeum</i> <i>Atopobium parvulum</i>	<i>Atopobium parvulum</i>
208	<i>Clostridium saccharolyticum</i> , <i>Roseburia hominis</i>	<i>Clostridiales genomu sp. BVAB3</i> <i>Clostridium saccharolyticum</i>
216	<i>Eubacterium eligen</i> <i>Butyrivibrio proteoclasticus</i> <i>Eubacterium eligens</i>	<i>Eubacterium limosum</i> <i>Eubacterium rectale</i>
224	ND	
269	<i>Ruminococcus albus</i>	
295	<i>Selenomonas ruminantium</i> <i>Megasphaera elsdenii</i> <i>Veillonella parvula</i>	<i>Acidaminococcus fermentans</i> <i>Acidaminococcus intestini</i>
316	<i>Oenococcus oeni</i>	
399	ND	
458	ND	
475	<i>Lactobacillus casei</i>	
485	<i>Prevotella buccalis</i>	
495	ND	
522	ND	
548	<i>Lactococcus garvieae</i> <i>Lactococcus lactis</i> <i>Leuconostoc citreum</i> <i>Leuconostoc mesenteroides</i> <i>Streptococcus sanguinis</i> <i>Streptococcus oralis</i> <i>Streptococcus macedonicus</i>	<i>Streptococcus mitis</i> <i>Streptococcus parasanguinis</i> <i>Streptococcus salivarius</i> <i>Streptococcus agalactiae</i> <i>Streptococcus infantarius</i> <i>Streptococcus suis</i> <i>Streptococcus thermophilus</i>

Table 3. Cont.

OTU	Predicted Bacteria from T-RFLP
558	<i>Enterococcus faecalis</i> <i>Lactobacillus salivarius</i> <i>Enterococcus casseliflavus</i>
	<i>Enterococcus sp. 7L76</i>

The bacterial list was selected from a study by Jin et al. (2014), and from the databases of CNGB (mouse and human) and MICA3.0 (RDP 16S Bacterial rRNA). The fragment pattern was simulated using the T-RFLP analysis program, MICA3.0 (<http://mica.ibest.uidaho.edu>, accessed on 1 March 2021), and a web-based simulation tool (<http://insilico.ehu.eus/T-RFLP/info.html>, accessed on 1 March 2021). ND indicates not detected. The bacterial list in this table is a prediction of possible species, but not the existence of bacteria in the sample.

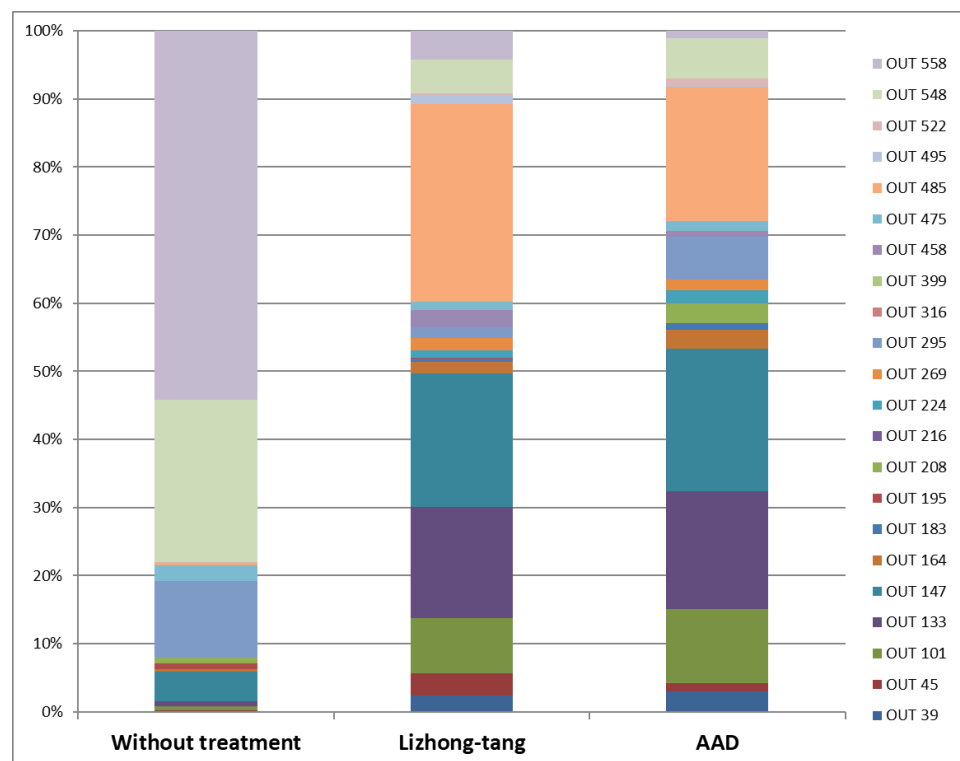


Figure 7. T-RFLP profiles of small intestinal contents, based on operational taxonomic units (OTUs). After the experiment, to assess the anti-diarrheal effect of *Lizhong-tang* on mice in an antibiotic-associated diarrhea (AAD) model induced by means of lincomycin oral administration, DNA was isolated from the feces-containing intestinal tissues of each mouse. The isolated DNA was analyzed using T-RFLP, with the help of CNGB (mouse and human) and MICA3.0 (RDP 16S bacterial rRNA) databases. Fragment pattern was simulated using the T-RFLP analysis program, MICA3.0 (<http://mica.ibest.uidaho.edu>, accessed on 1 March 2021), and a web-based simulation tool (<http://insilico.ehu.eus/T-RFLP/info.html>, accessed on 1 March 2021). Normal group: without treatment. Control group: AAD group. Sample group: *Lizhong-tang*-administered group, post-AAD establishment.

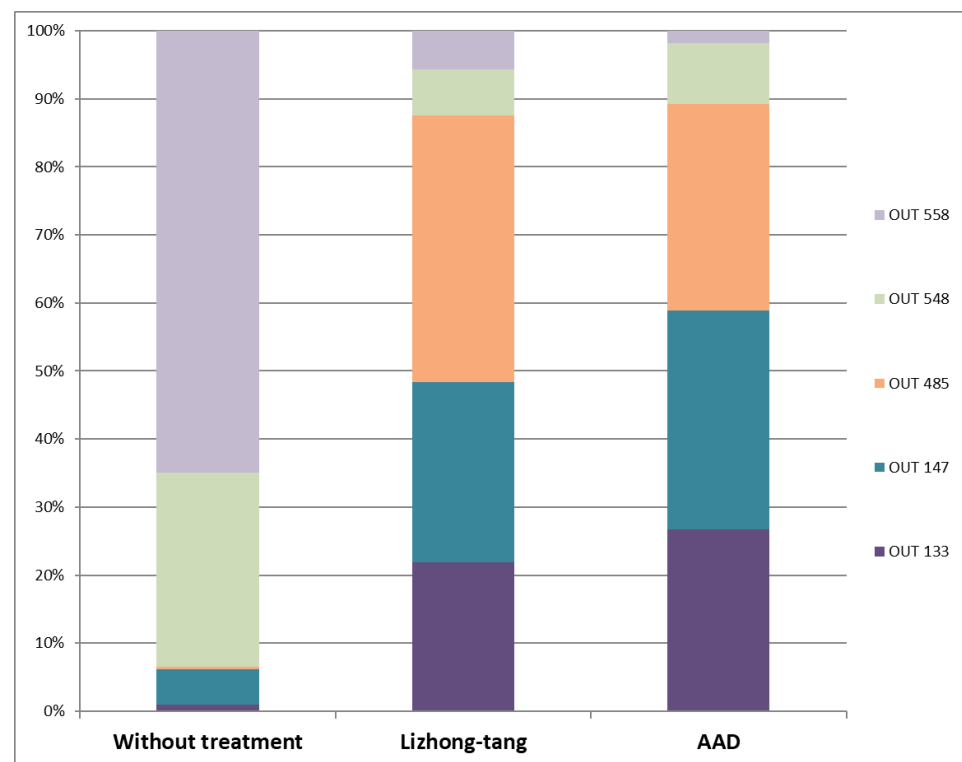


Figure 8. Comparison of operational taxonomic units (OTUs) 133, 147, 485, 548, and 558 between the normal, control, and *Lizhong-tang*-administered groups. After the in vivo experiment (to assess the anti-diarrheal effect of *Lizhong-tang* on mice in an antibiotic-associated diarrhea (AAD) model induced by means of lincomycin oral administration), DNA was isolated from the feces-containing intestinal tissues of each mouse. Microbiome analysis was carried out using the T-RFLP method. N1–N5: normal groups (groups not given any treatment). E1–E5: sample groups (in these groups, *Lizhong-tang* was orally administered to the animals, post-AAD establishment), C1–C5: control groups (AAD groups).

4. Discussion

In this study, we investigated whether antibiotic-induced changes in intestinal microflora could be readjusted using herbal medicines [23]. We reviewed 25 experimental studies related to intestinal microbes in Eastern medicine in terms of the effects of intestinal microbe-related diseases, research subjects used in experiments, methods of establishing experimental models for each disease, drugs used in the experiments, and herbal medicines [24]. Among the studies on the gut microbiome, Ryu et al. [25] reported the role and function of gut microbes from a pediatric point of view, with a focus on gut microbes and oriental medicine research. Experimental studies have analyzed the role of intestinal microbes in metabolic diseases, related to the intestine, such as diabetes [26–29], obesity [30–33], irritable bowel syndrome [34,35], and intestinal inflammatory diseases [36,37]. Several studies have also analyzed the effect of herbal medicines on the imbalance of intestinal microflora caused by antibiotics [16–19], but they are limited to some prescriptions and individual drugs and have not been reported in Korea.

Therefore, in this study, before examining the effects of herbal medicines on antibiotic-induced changes, we selected 10 herbal medicinal extracts with anti-inflammatory effects through an in vitro experiment. Since it is difficult to experimentally test diarrhea in vitro, we wanted to find a drug that can improve diarrhea from various herbal medicines with anti-inflammatory effects. Further experiments were performed to investigate their mechanism of action. In the in vivo experiment, we selected an herbal extract with an anti-inflammatory effect, and elucidated its anti-diarrheal effect on the AAD mouse model and analyzed its effect on the intestinal microflora. Three prescriptions (*Lizhong-tang*, *Osuyu-tang*, and

Oryeong-san) and seven herbal medicines (*Atractylodes japonica* Koidz, *Coix lacryma-jobi*, *Angelica dahurica*, *Cinamomum cassia*, *Aucklandiae radix*, and *Machilus thunbergii*) were selected because they displayed anti-inflammatory, -digestive, and -diarrheal effects [20,21].

Antibiotics not only kill pathogenic bacteria, but also eliminate normal gut microbes, which allows harmful bacteria to multiply. In particular, *Clostridium difficile* proliferates excessively in the intestine, damages the intestinal wall, and produces chemicals that cause enteritis, abdominal pain, and diarrhea [38,39]. Diarrhea can be alleviated by inhibiting inflammation; thus, the inhibitory effect of 10 herbal medicines on NO production was first evaluated by means of an in vitro experiment. The results showed that *M. thunbergii* and *Lizhong-tang* exhibited no cytotoxicity and the best activity at 100 µg/mL concentration (Figure 2). Immune response occurs in macrophages and produces free radicals (such as NO) and cytokines (such as IL-6 and TNF-α). NO is a highly reactive oxygen species that mediates vasodilation and signal transduction in the human body [40,41]. Therefore, inhibition of NO production decreases the anti-inflammatory response.

Since *Lizhong-tang* displayed the highest anti-inflammatory effect among the 10 drugs, we investigated the inhibition of NO production by the different active compounds of *Lizhong-tang* further to determine the mechanism of inhibition of inflammation. Among the active compounds of *Lizhong-tang*, liquiritin and 6-gingerol had the highest NO inhibitory effect, and upon simultaneous treatment with liquiritin and 6-gingerol, they inhibited NO production as much as the sum of the NO inhibitory effects of each sample (Figures 3 and 4). When an intracellular inflammatory response occurs, NF-κB is activated, which affects various cellular signaling molecules. Representative signals that affect its activation include JNK, ERK, and p38 MAPK [42]. They are unphosphorylated in the cytoplasm but are phosphorylated and translocated to the nucleus upon stimulation by LPS. In addition, NF-κB is known to be a transcriptional regulator that induces the expression of mediators related to inflammation. When activated by LPS, NF-κB is involved in the expression of genes such as *iNOS*, *COX-2*, and pro-inflammatory cytokines [43–45]. Therefore, to investigate whether liquiritin and 6-gingerol affected the activation of phosphorylated *iNOS*, *COX-2* MAPKs, an increase in the phosphorylation of *iNOS*, *COX-2* MAPKs was confirmed by Western blotting following LPS stimulation. In addition, the effects of liquiritin and 6-gingerol treatment on the expression of *iNOS* and *COX-2* in the cytoplasm of RAW 264.7 cells were also analyzed (Figure 5). The active compounds of *Lizhong-tang*, liquiritin and 6-gingerol, were found to inhibit LPS-activated JNK, ERK, and p38 MAPK expression, and inhibiting *iNOS* and *COX-2* expression.

Mice are the most widely used animal species for the modeling of acute and chronic diseases. Additionally, as in humans, the mouse gut microbiome is stable and resilient. Therefore, mouse model studies are often used to investigate the relationship between gut microbiota and disease [40,41,46,47]. In the present study, animal experiments were performed to investigate the effects and control of intestinal microflora induced by *Lizhong-tang* and *M. officinalis* extracts in AAD. The effect of herbal medicines in a mouse model induced by antibiotic administration was investigated by measuring weight change, water intake, and diarrhea status score of the mice. In the control group, which was a model of AAD, sustained weight loss was observed while water intake increased. Similar to the untreated group (normal), the *Lizhong-tang*-treated group showed almost no weight change, with the greatest improvement in diarrheal symptoms (Table 2). Although *Lizhong-tang* relieved AAD symptoms through gastrointestinal function control, body weight initially reduced due to the decrease in diarrhea but recovered rapidly thereafter. Thus, it can be concluded that *Lizhong-tang* was effective in improving AAD.

Microbial analysis generates OTU tables based on sequence groups through noise filtering, sorting, and bulk sequence classification, and then compares them with sample information to perform diversity and network analyses [48]. In this study, changes in the intestinal microflora were observed upon the administration of antibiotics and *Lizhong-tang*. Compared to the control group, in which only antibiotics were administered, there was a change in the intestinal microflora in the *Lizhong-tang*-administered group (Figures 7 and 8).

This suggests that *Lizhong-tang* can alleviate diarrheal symptoms by controlling the composition and diversity of intestinal microbes induced by antibiotics. The mammalian gut microbiota consists of a complex bacterial community of at least 1000 species, most of which belong to the phyla Bacteroidetes and Firmicutes. The phylum Bacteroidetes is Gram-negative and includes *Bacteroides*, *Cytophaga*, *Flavobacterium*, whereas the phylum Firmicutes has Gram-positive bacteria, which includes Enterococcaceae, Lactobacillaceae, and Clostridia [49,50]. Macrolides have been reported to decrease *Actinobacteria* and increase *Bacteroides* and *Proteobacteria* by altering intestinal microflora. In addition, vancomycin has been shown to decrease *Firmicutes* in feces, increase *Proteobacteria*, and decrease microbial diversity [51].

Although this study is aimed at screening the efficacy of herbal preparations, there are some limitations in animal experiments that need to be considered in the future studies. Adequate period of time was not selected to give effects to such bacteria colonize the gut and contribute to gut homeostasis. In addition, there was a lack of confirmation of changes in inflammation and intestinal structure. Finally, research on an appropriate positive control group, which is not yet available, should be conducted.

5. Conclusions

AAD is associated with intestinal microbiome imbalance, inflammation, and changes in intestinal structure. We screened herbal medicines showing anti-inflammatory effects and looked for materials that improved diarrhea among drugs with anti-inflammatory effects. The results of this study confirm that *Lizhong-tang* is effective against AAD and that both its active compounds (liquiritin and 6-gingerol) could have a beneficial effect on the intestinal environment by altering the intestinal microbial community. *Lizhong-tang* exhibits anti-inflammatory effects by inhibiting the expression of iNOS and COX-2, showing the potential to suppress inflammation caused by ADD. As research on the development of probiotics progresses, Eastern medicine could provide compounds that show potential as therapeutic agents to improve the intestinal environment.

Author Contributions: Conceptualization, K.S.K. and H.L.L.; methodology, H.-R.A. and Q.N.N.; formal analysis, D.-W.K., J.Y.P., M.-S.S. and Q.N.N.; investigation H.-R.A. and D.H.P.; writing—original draft preparation, H.-R.A. and D.H.P.; writing—review and editing, K.S.K. and H.L.L.; project administration, K.S.K.; funding acquisition, H.L.L. All authors have read and agreed to the published version of the manuscript.

Funding: This research was supported by the Daejeon University fund (2021). This research was supported by the Basic Science Research Program through the National Research Foundation of Korea, funded by the Ministry of Education (2020M3A9E410438012).

Conflicts of Interest: The authors declare no conflict of interest.

References

1. Peterson, J.; Garges, S.; Giovanni, M.; McInnes, P.; Wang, L.; Schloss, J.A.; Bonazzi, V.; McEwen, J.E.; Wetterstrand, K.A.; Deal, C. The NIH human microbiome project. *Genome Res.* **2009**, *19*, 2317–2323. [[PubMed](#)]
2. Ko, J.S. The intestinal microbiota and human disease. *Korean J. Gastroenterol.* **2013**, *62*, 85–91. [[CrossRef](#)]
3. Tanaka, M.; Nakayama, J. Development of the gut microbiota in infancy and its impact on health in later life. *Allergol. Int.* **2017**, *66*, 515–522. [[CrossRef](#)] [[PubMed](#)]
4. Koenig, J.E.; Spor, A.; Scalfone, N.; Fricker, A.D.; Stombaugh, J.; Knight, R.; Angenent, L.T.; Ley, R.E. Succession of microbial consortia in the developing infant gut microbiome. *Proc. Natl. Acad. Sci. USA* **2011**, *108*, 4578–4585. [[CrossRef](#)] [[PubMed](#)]
5. Mueller, N.T.; Whyatt, R.; Hoepner, L.; Oberfield, S.; Dominguez-Bello, M.G.; Widen, E.; Hassoun, A.; Perera, F.; Rundle, A. Prenatal exposure to antibiotics, cesarean section and risk of childhood obesity. *Int. J. Obes.* **2015**, *39*, 665–670. [[CrossRef](#)] [[PubMed](#)]
6. Macpherson, A.J.; de Agüero, M.G.; Ganai-Vonarburg, S.C. How nutrition and the maternal microbiota shape the neonatal immune system. *Nat. Rev. Immunol.* **2017**, *17*, 508–517. [[CrossRef](#)] [[PubMed](#)]
7. Lee, E.J.; Kim, H.J.; Lee, S.H.; Chang, G.T. The relationship between children's temperament and character to functional gastrointestinal disorders. *J. Pediatr. Korean Med.* **2015**, *29*, 60–68. [[CrossRef](#)]

8. Lutgendorff, F.; Akkermans, L.; Soderholm, J.D. The role of microbiota and probiotics in stress-induced gastrointestinal damage. *Curr. Mol. Med.* **2008**, *8*, 282–298. [[CrossRef](#)]
9. Kardas, P.; Devine, S.; Golembesky, A.; Roberts, C. A systematic review and meta-analysis of misuse of antibiotic therapies in the community. *Int. J. Antimicrob. Agents* **2005**, *26*, 106–113. [[CrossRef](#)]
10. McFarland, L.V.; Beneda, H.W.; Clarridge, J.E.; Raugi, G.J. Implications of the changing face of *Clostridium difficile* disease for health care practitioners. *Am. J. Infect. Control.* **2007**, *35*, 237–253. [[CrossRef](#)]
11. Spellberg, B.; Gidos, R.; Gilbert, D.; Bradley, J.; Boucher, H.W.; Scheld, W.M.; Bartlett, J.G.; Edwards, J., Jr.; Infectious Diseases Society of America. The epidemic of antibiotic-resistant infections: A call to action for the medical community from the Infectious Diseases Society of America. *Clin. Infect. Dis.* **2008**, *46*, 155–164. [[CrossRef](#)]
12. OECD. OECD Health Data. 2021. Available online: <https://stats.oecd.org/Index.aspx?ThemeTreeId=9> (accessed on 1 March 2021).
13. Mueller, N.T.; Bakacs, E.; Combellick, J.; Grigoryan, Z.; Dominguez-Bello, M.G. The infant microbiome development: Mom matters. *Trends Mol. Med.* **2015**, *21*, 109–117. [[CrossRef](#)] [[PubMed](#)]
14. An, X.; Bao, Q.; Di, S.; Zhao, Y.; Zhao, S.; Zhang, H.; Lian, F.; Tong, X. The interaction between the gut microbiota and herbal medicines. *Biomed. Pharmacother.* **2019**, *118*, 109252. [[CrossRef](#)] [[PubMed](#)]
15. Francino, M.P. Early development of the gut microbiota and immune health. *Pathogens* **2014**, *3*, 769–790. [[CrossRef](#)] [[PubMed](#)]
16. Bäckhed, F.; Ding, H.; Wang, T.; Hooper, L.V.; Koh, G.Y.; Nagy, A.; Semenkovich, C.F.; Gordon, J.I. The gut microbiota as an environmental factor that regulates fat storage. *Proc. Natl. Acad. Sci. USA* **2004**, *101*, 15718–15723. [[CrossRef](#)] [[PubMed](#)]
17. Liu, C.; Zhang, C.; Lv, W.; Chao, L.; Li, Z.; Shi, D.; Guo, S. Structural modulation of gut microbiota during alleviation of suckling piglets diarrhoea with herbal formula. *Evid.-Based Complementary Altern. Med.* **2017**, *2017*, 8358151. [[CrossRef](#)]
18. Xie, G.; Wu, Y.; Zheng, T.; Shen, K.; Tan, Z. Effect of *Debaryomyces hansenii* combined with Qiweibaizhu powder extract on the gut microbiota of antibiotic-treated mice with diarrhea. *3 Biotech* **2020**, *10*, 127. [[CrossRef](#)]
19. Qu, Q.; Yang, F.; Zhao, C.; Liu, X.; Yang, P.; Li, Z.; Han, L.; Shi, X. Effects of fermented ginseng on the gut microbiota and immunity of rats with antibiotic-associated diarrhea. *J. Ethnopharmacol.* **2021**, *267*, 113594. [[CrossRef](#)]
20. Dethlefsen, L.; Relman, D.A. Incomplete recovery and individualized responses of the human distal gut microbiota to repeated antibiotic perturbation. *Proc. Natl. Acad. Sci. USA* **2011**, *108*, 4554–4561. [[CrossRef](#)]
21. Lee, J.H.; Oh, J. A Comparative Analysis about Various Editions of Donguibogam. *J. Korean Med. Hist.* **2015**, *23*, 235–243.
22. Seo, C.-S.; Kim, O.S.; Kim, Y.; Shin, H.-K. Quantification Analysis and Antioxidant Activity of Leejung-tang. *Herb. Formula Sci.* **2013**, *21*, 177–185. [[CrossRef](#)]
23. Clemente, J.C.; Ursell, L.K.; Parfrey, L.W.; Knight, R. The impact of the gut microbiota on human health: An integrative view. *Cell* **2012**, *148*, 1258–1270. [[CrossRef](#)] [[PubMed](#)]
24. Ahn, H.R.; Song, J.H.; Lee, H.L. A Review of the Experimental Studies on the Modulatory Effect Herbal Medicine on Gut Microbiota. *J. Pediatrics Korean Med.* **2020**, *34*, 43–58.
25. Ryu, D.; Kim, K. Current trends and future directions of gut microbiota and their-derived metabolite study in the pediatric perspective of Korean medicine. *J. Pediatrics Korean Med.* **2019**, *33*, 34–45.
26. Han, L.; Li, T.; Du, M.; Chang, R.; Zhan, B.; Mao, X. Beneficial effects of potentilla discolor bunge water extract on inflammatory cytokines release and gut microbiota in high-fat diet and streptozotocin-induced type 2 diabetic mice. *Nutrients* **2019**, *11*, 670. [[CrossRef](#)]
27. Cao, Y.; Yao, G.; Sheng, Y.; Yang, L.; Wang, Z.; Yang, Z.; Zhuang, P.; Zhang, Y. JinQi Jiangtang tablet regulates gut microbiota and improve insulin sensitivity in type 2 diabetes mice. *J. Diabetes Res.* **2019**, *2019*, 1872134. [[CrossRef](#)]
28. Chen, M.; Liao, Z.; Lu, B.; Wang, M.; Lin, L.; Zhang, S.; Li, Y.; Liu, D.; Liao, Q.; Xie, Z. Huang-Lian-Jie-Du-decoction ameliorates hyperglycemia and insulin resistant in association with gut microbiota modulation. *Front. Microbiol.* **2018**, *9*, 2380. [[CrossRef](#)]
29. Gu, W.; Yang, M.; Bi, Q.; Zeng, L.-X.; Wang, X.; Dong, J.-C.; Li, F.-J.; Yang, X.-X.; Li, J.-P.; Yu, J. Water extract from processed *Polygonum multiflorum* modulate gut microbiota and glucose metabolism on insulin resistant rats. *BMC Complementary Med. Ther.* **2020**, *20*, 107. [[CrossRef](#)]
30. Gong, S.; Ye, T.; Wang, M.; Wang, M.; Li, Y.; Ma, L.; Yang, Y.; Wang, Y.; Zhao, X.; Liu, L. Traditional Chinese medicine formula Kang Shuai Lao Pian improves obesity, gut dysbiosis, and fecal metabolic disorders in high-fat diet-fed mice. *Front. Pharmacol.* **2020**, *11*, 297. [[CrossRef](#)]
31. Zhang, C.; Liu, J.; He, X.; Sheng, Y.; Yang, C.; Li, H.; Xu, J.; Xu, W.; Huang, K. Caulis spatholobi ameliorates obesity through activating brown adipose tissue and modulating the composition of gut microbiota. *Int. J. Mol. Sci.* **2019**, *20*, 5150. [[CrossRef](#)]
32. Park, J.-H.; Kim, H.-J.; Lee, M.-J. The role of gut microbiota in obesity and utilization of fermented herbal extracts. *J. Korean Med. Obes. Res.* **2009**, *9*, 1–14.
33. Hussain, A.; Yadav, M.K.; Bose, S.; Wang, J.-H.; Lim, D.; Song, Y.-K.; Ko, S.-G.; Kim, H. Daesihotang is an effective herbal formulation in attenuation of obesity in mice through alteration of gene expression and modulation of intestinal microbiota. *PLoS ONE* **2016**, *11*, e0165483. [[CrossRef](#)] [[PubMed](#)]
34. Chen, Y.; Xiao, S.; Gong, Z.; Zhu, X.; Yang, Q.; Li, Y.; Gao, S.; Dong, Y.; Shi, Z.; Wang, Y. Wuji Wan formula ameliorates diarrhea and disordered colonic motility in post-inflammation irritable bowel syndrome rats by modulating the gut microbiota. *Front. Microbiol.* **2017**, *8*, 2307. [[CrossRef](#)] [[PubMed](#)]

35. Li, J.; Cui, H.; Cai, Y.; Lin, J.; Song, X.; Zhou, Z.; Xiong, W.; Zhou, H.; Bian, Y.; Wang, L. Tong-Xie-Yao-Fang regulates 5-HT level in diarrhea predominant irritable bowel syndrome through gut microbiota modulation. *Front. Pharmacol.* **2018**, *9*, 1110. [[CrossRef](#)] [[PubMed](#)]
36. Zhang, Z.; Cao, H.; Shen, P.; Liu, J.; Cao, Y.; Zhang, N. Ping weisan alleviates chronic colitis in mice by regulating intestinal microbiota composition. *J. Ethnopharmacol.* **2020**, *255*, 112715. [[CrossRef](#)] [[PubMed](#)]
37. Wu, Z.-c.; Zhao, Z.-l.; Deng, J.-p.; Huang, J.-t.; Wang, Y.-f.; Wang, Z.-p. Sanhuang Shu'ai decoction alleviates DSS-induced ulcerative colitis via regulation of gut microbiota, inflammatory mediators and cytokines. *Biomed. Pharmacother.* **2020**, *125*, 109934. [[CrossRef](#)]
38. Sun, Y.-F.; Zhang, X.; Wang, X.-Y.; Jia, W. Effect of long-term intake of ginseng extracts on gut microbiota in rats. *China J. Chin. Mater. Med.* **2018**, *43*, 3927–3932.
39. Isolauri, E.; Salminen, S. Probiotics, gut inflammation and barrier function. *Gastroenterol. Clin.* **2005**, *34*, 437–450. [[CrossRef](#)]
40. Malakoff, D. The rise of the mouse, biomedicine's model mammal. *Science* **2000**, *288*, 248–253. [[CrossRef](#)]
41. Schellinck, H.M.; Cyr, D.P.; Brown, R.E. How many ways can mouse behavioral experiments go wrong? Confounding variables in mouse models of neurodegenerative diseases and how to control them. In *Advances in the Study of Behavior*; Elsevier: Amsterdam, The Netherlands, 2010; Volume 41, pp. 255–366.
42. McFarland, L.V. Normal flora: Diversity and functions. *Microb. Ecol. Health Dis.* **2000**, *12*, 193–207.
43. Lowenstein, C.J.; Dinerman, J.L.; Snyder, S.H. Nitric oxide: A physiologic messenger. *Ann. Intern. Med.* **1994**, *120*, 227–237. [[CrossRef](#)] [[PubMed](#)]
44. Moncada, S. Nitric oxide: Physiology, pathophysiology and pharmacology. *Pharmacol. Rev.* **1991**, *43*, 109–142. [[PubMed](#)]
45. Guha, M.; Mackman, N. LPS induction of gene expression in human monocytes. *Cell. Signal.* **2001**, *13*, 85–94. [[CrossRef](#)]
46. Ki, S.H.; Choi, M.J.; Lee, C.H.; Kim, S.G. Gα12 specifically regulates COX-2 induction by sphingosine 1-phosphate: Role for JNK-dependent ubiquitination and degradation of IκBα. *J. Biol. Chem.* **2007**, *282*, 1938–1947. [[CrossRef](#)]
47. Dong, C.; Davis, R.J.; Flavell, R.A. MAP kinases in the immune response. *Annu. Rev. Immunol.* **2002**, *20*, 55–72. [[CrossRef](#)]
48. Gurfein, B.T.; Stamm, A.W.; Bacchetti, P.; Dallman, M.F.; Nadkarni, N.A.; Milush, J.M.; Touma, C.; Palme, R.; Di Borgo, C.P.; Fromentin, G. The calm mouse: An animal model of stress reduction. *Mol. Med.* **2012**, *18*, 606–617. [[CrossRef](#)]
49. Hooper, L.V.; Macpherson, A.J. Immune adaptations that maintain homeostasis with the intestinal microbiota. *Nat. Rev. Immunol.* **2010**, *10*, 159–169. [[CrossRef](#)]
50. Korpela, K.; Salonen, A.; Virta, L.J.; Kekkonen, R.A.; Forslund, K.; Bork, P.; De Vos, W.M. Intestinal microbiome is related to lifetime antibiotic use in Finnish pre-school children. *Nat. Commun.* **2016**, *7*, 10410. [[CrossRef](#)]
51. Isanaka, S.; Guindo, O.; Langendorf, C.; Matar Seck, A.; Plikaytis, B.D.; Sayinzoga-Makombe, N.; McNeal, M.M.; Meyer, N.; Adehossi, E.; Djibo, A. Efficacy of a low-cost, heat-stable oral rotavirus vaccine in Niger. *N. Engl. J. Med.* **2017**, *376*, 1121–1130. [[CrossRef](#)]